07,01

The effect of thermomechanical effects on nanoscale discontinuities and mechanical properties of an amorphous Ni-based alloy obtained by ultrafast quenching

© A.G. Kadomtsev, M.V. Narykova, V.I. Betekhtin, O.V. Amosova

Ioffe Institute,
St. Petersburg, Russia

E-mail: Andrej.Kadomtsev@mail.ioffe.ru

Received July 12, 2023
Revised July 12, 2023
Accepted July 13, 2023

The effect of thermomechanical treatment on the parameters of discontinuities of excess free volume and a complex of mechanical properties has been studied for amorphous tapes with a thickness of $\sim 70\,\mu$m obtained by ultrafast quenching. The features of the influence of excess free volume on the properties and stability of an amorphous alloy of increased volume (thickness) are analyzed.

Keywords: amorphous alloys, free volume, pressure, annealing, mechanical properties, excess free volume.

DOI: 10.61011/PSS.2023.11.57325.147

1. Introduction

Amorphous alloys (AA), produced by ultrafast quenching (UFQ) from a melt, have useful physical and mechanical properties (magnetic characteristics, high strength, hardness, etc.) and are therefore used in a number of state-of-the-art technologies [1–6]. One of the important disadvantages of these alloys is their mechanical-thermal instability, resulting in degradation of these properties during long-term operation. This instability is associated with the relaxation of part of the huge energy introduced into the alloys in the process of UFQ and manifests in a change in their free volume. The concept of free volume [7–10] is based on the fact that the density of an AA is approximately 2% less than that of its crystalline equivalent.

In [5,11–13], an assumption is made that in the general case the free volume of an AA can be divided into structurally determined free volume and excess free volume (EFV). The structural component of the free volume is an integral characteristic of the amorphous state, atomic complexes that determine the topological as well as compositional characteristics of the amorphous state. It is completely removed only after the amorphous alloy transforms into a crystalline state, for example, when heated to the crystallization temperature. The description in terms of excess free volume does not impose restrictions on the structural model of the natural amorphous state. The EFV can be considered as a structural defect (a nanoscale region of reduced density, in the extreme case — nanopores). EFV parameters and their evolution can have a significant effect on the properties of amorphous alloys [6,13–15].

It seems that the physical nature of the formation of low-density regions after UFQ can be associated with the ideas of S.M. Frenkel [16], according to which liquid metals contain many nanoscale regions of low density that one moment are formed, then the next moment are healed. Thus, the amorphous alloy resulted from UFQ „inherits“ the defective structure of its liquid state. With this approach, the temperature of the liquid alloy should affect the EFV parameters; an increase in this temperature intensifies the process of evolution of low-density regions. In [14], it was found that an increase in the temperature of the liquid alloy leads to a noticeable increase in the EFV regions formed after UFQ.

In a number of studies, using the method of small-angle X-ray scattering (SAXS), the shape of the EFV, their bimodal distribution by sizes (~ 100 and ~ 30 nm) were determined, and most importantly, the effect of thermobaric impact on EFV parameters and, as a consequence, on the physical and mechanical properties of a number of amorphous alloys based on Fe, Co [6–12]. All these studies were carried out mainly for fairly thin ($\sim 20-30\,\mu$m) amorphous tapes.

In this study, for the first time, all EFV parameters and their evolution under thermomechanical impact, as well as the relationship of this evolution with mechanical properties, were determined for significantly thicker ($\sim 70\,\mu$m) amorphous alloy tapes. It seemed that an increase in the volume of the amorphous alloy under study (approximately by three times) would make it possible to obtain new information about the nature of the effect of EFV parameters on the alloy properties and, on this basis, on the methods and ways of increasing the mechanical and thermal stability of these high-strength materials. The data obtained may be useful when using larger products with amorphous structure in practice.

2. Materials and research methods

In our study, we were focused on the $Ni_{82.1}Cr_{7.8}Si_{4.6}Fe_{3.1}Mn_{0.3}Al_{0.1}Cu< 0.1B_2$ amorphous

alloy. It seems that the complex chemical composition of this alloy has become one of the important factors in producing fairly „thick“ ($\sim 65-75\,\mu$m) amorphous tapes after UFQ. 20×10 mm rectangular sections were cut out from the resulting tapes, from which samples with a shape of „figure of eight“ with a quasi-homogeneous part length of 8 mm and a minimum width of 3 mm were prepared using a special set-up.

The samples were mechanically tested under conditions of their stretching until break under loading with a constant rate of increase in the applied stress of 25 MPa/s. Before testing, the samples were carefully centered in the testing machine. This made it possible to reduce the spread in values of the tensile strength σ_r to 5% from sample to sample. Heat treatment of the samples before testing was carried out under annealing conditions in a temperature range of 293–623 K; the annealing time at each temperature was 5 h. For the purpose of baric treatment, the samples were placed in a metal capsule with an oil medium and subjected to a hydrostatic pressure of 1 GPa for 15 min at 293 K in a special „bomb“. Density ρ of the samples and its evolution after thermal exposure were determined by hydrostatic weighing with an accuracy of 10^{-4}%. Young's modulus E was measured by the electrostatic method using bending vibrations [17].

The parameters of inhomogeneous density areas, such as EFV regions, were measured by the small-angle X-ray scattering (SAXS) method on a modernized X-ray set-up with Kratky collimation using MoK_α- radiation. By varying the X-ray beam width from 4 to 120 μm, electron density inhomogeneities were recorded in the size range from a few nanometers to ~ 300 nm. The SAXS data were processed both by the Guinier tangent curves method [18] and by plotting and analyzing invariants of the SAXS indicatrix [19].

All SAXS measurements were carried out for amorphous tapes produced after UFQ and exposure to high hydrostatic pressure, which makes it possible to identify the „void“ nature of electron density inhomogeneities [6].

3. Results of the studies and their analysis

First of all, let us consider the data on the dependence of strength (tensile strength σ_r at 293 K) on the preliminary annealing temperature (Figure 1). It can be seen that this dependence is non-monotonic. With increasing annealing temperature, the strength first increases and at 510 K reaches its greatest value, and in the interval of 515–595 K the σ_r decreases slightly and partially stabilizes. At $T \geq 600$ K the strength drops sharply. The dependence of microhardness H on the annealing temperature has a similar behavior. Up to a pre-annealing temperature of 510 K, the H (at 293 K) increases, and in the region of 510–600 K a diffused maximum of H is observed.

The strongest effect of annealing on the strength was observed for the samples annealed in a field of mechanical forces. Thus, for the samples that, during annealing at

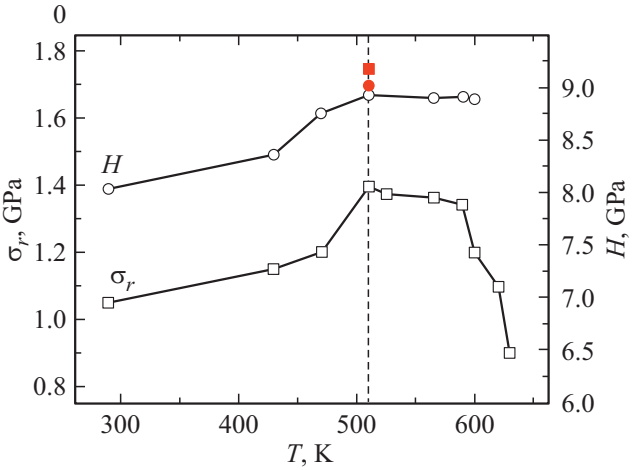

Figure 1. Dependence of tensile strength σ_r and microhardness H on annealing temperature. Solid symbols indicate σ_r after annealing under load (squares) and H after exposure to hydrostatic pressure (circles) at a temperature of 510 K.

510 K, were under the action of a tensile load of ~ 80% of the tensile strength at this temperature, the strength after testing at 293 K increased sharply (Figure 1). (The tensile load was determined after break of the samples at 510 K).

Taking into account the fact that the greatest effect on σ_r and H has the annealing at 510 K and especially the annealing at this temperature under load, the effect of these treatment methods on the modulus of elasticity E and density ρ of the amorphous alloy were investigated in this study.

As a result of a comprehensive study, values of σ_r, H, E, ρ were obtained for four states of the amorphous alloy: the initial state (after UFQ); the state after annealing at the optimal (for increasing σ_r) temperature of 510 K; the state after annealing at the same temperature under load; the state after exposure of the alloy in the initial state to high hydrostatic pressure (Table 1). Table 1 also shows estimates of the change in density $\Delta\rho/\rho$ after processing the alloy by the methods described above.

It is clear rom Table 1 that it is the magnitude of the decompaction $\Delta\rho/\rho$ resulted from thermomechanical treatments that determines the effect of increasing (compared to the initial state) the values of σ_r, H, E. And the value of $\Delta\rho/\rho$ is important and not the method of affecting the density, which results in a decrease in $\Delta\rho/\rho$. Thus, the value of $\Delta\rho/\rho$ turned out to be almost the same after annealing at 510 K and after exposure to hydrostatic pressure ($1.37 \cdot 10^{-2}$ and $1.34 \cdot 10^{-2}$, respectively). The values of σ_r also turned out to be close (1.4 GPa and 1.39 GPa, respectively).

Some features of the effect of various processing methods on the elastic modulus are worth noting. It can be seen from Table 1 that after thermomechanical treatment the modulus naturally increases, and after exposure to hydrostatic pressure it decreased and became even lower than in the initial state. A similar effect was previously

Table 1. Parameters of the amorphous alloy in various states

Studied parameters of material	After UFQ	After annealing at 510 K	After annealing at 510 K under load of $0.8\sigma_r$	After exposure to hydrostatic pressure of 1 GPa
σ, GPa	1.05	1.4	1.7	1.39
H, GPa	8.03	8.92	9.0	9.23
E, GPa	183	204	220	180
ρ	7.734	7.84	7.857	7.838
$\Delta\rho/\rho$	–	$1.37 \cdot 10^{-2}$	$1.59 \cdot 10^{-2}$	$1.34 \cdot 10^{-2}$

observed by the authors when studying thin ($\sim 20\,\mu$m) amorphous tapes [6].

It seems that this modulus change effect is due to the following factors.

As the temperature (of annealing) increases, the initial (after UFQ) internal stresses decrease and discontinuities begin to heal. The healing, as shown by thermal activation analysis, is explained by the viscous flow of the amorphous structure stimulated by the elevated temperature [20].

When pressure is applied, an additional increase in stress is added to the UFQ. Such stresses, as shown by analysis from the standpoint of the nonlinear theory of elasticity, arise on the surface of discontinuities (such as pores), the shape of which differs from the „ideal" sphere [21]. The resulting additional stresses lead to elastic and quasi-plastic deformations (localized shears), stimulating the healing.

The elastic-plastic shears that occur under pressure on the surface of discontinuities lead, possibly, to the formation of crystallization centers detected by atomic-force microscopy [15].

A more noticeable increase in H after the action of hydrostatic pressure (compared to the change in H during annealing under load) may be associated with the appearance of crystallization centers on the surface of the discontinuity (Table 1, Figure 1)

Let us summarize the preliminary results of the experiments described above. It can be seen from Table 1 that there is a clear connection between the change in the density growth under thermomechanical and baric impacts and the increase in the values of the mechanical characteristics (σ_r, H) of the amorphous alloy. To clarify the physical nature of these changes, it is important to identify factors leading to an increase in density and, above all, the free volume, which is typical for the amorphous state. Our X-ray studies have unambiguously shown that the Ni-based alloy tapes with a thickness of $70\,\mu$m after UFQ are in an amorphous state. This amorphous state remains even after exposure to the thermomechanical and baric impacts used in the study. It should be noted that some results of this kind were obtained and analyzed for „thin" (with a thickness of $20-30\,\mu$m) tapes of amorphous alloys based on Fe and Co [6,12].

The obtained data on the stability of the amorphous state suggests that changes in the density of the alloy under study (Table 1) are obviously not associated with changes in the structurally determined free volume of the amorphous state.

In this case, it is natural to associate the decrease in density (increase in $\Delta\rho$) with the healing of nanoscale discontinuities that determine the EFV due to a decrease in their size. Information of this kind was also obtained by the method of small-angle X-ray scattering in the study of thin (with a thickness of $20-30\,\mu$m) tapes of amorphous alloys.

In this study, using SAXS, a complete assessment was carried out not only of the size, but also of the concentration of EFV elements for amorphous alloy samples that were sufficiently large in terms of the volume (thickness) under study. This made it possible to analyze the physical mechanisms of transformation of EFV parameters during UFQ and additional mechanothermal and baric treatment of samples of an amorphous alloy with a thickness of $\sim 70\,\mu$m.

Let us proceed to the consideration and analysis of the results of studying amorphous tapes with a thickness of $\sim 70\,\mu$m using the small-angle X-ray scattering method. These studies were carried out with the aim to identify nanoscale regions of reduced density and determine their parameters. To establish the relation between the data of structural studies and the results of mechanical tests (Table 1), the SAXS data was also obtained for four states of the amorphous alloy: the initial state (after UFQ), the state after annealing at 510 K in the free condition and under load, as well as the state after exposure to high hydrostatic pressure.

Figure 2 shows the invariants of the scattering indicatrix for the alloy in the initial (after UFQ) state and the same alloy after exposure to pressure. Processing the invariant according to [19] made it possible, even for the initial state of the alloy, to confidently identify two maxima associated with inhomogeneities having characteristic sizes of ~ 160 and 40 nm.

It can be seen from Figure 2 that the application of high hydrostatic pressure has resulted in a general decrease in the scattering intensity and a shift of the maxima towards smaller sizes of inhomogeneities.

Similar results of the effect on the size of nanoscale regions of reduced density were also obtained after impact on amorphous tapes with a thickness of $70\,\mu$m during annealing at 510 K in a free state and under load (Figure 3).

It can be seen from Figure 3 that annealing, and especially annealing under load, also leads to a decrease in the intensity of small-angle scattering. The processing by the

Table 2. Dimensions $D_{1,2}$ and concentration $N_{1,2}$ of inhomogeneities in samples of the $Ni_{82.1}Cr_{7.8}Si_{4.6}Fe_{3.1}Mn_{0.3}Al_{0.1}Cu_{<0.1}B_2$ amorphous alloy in various states

Samples	Large pores		Small pores	
	D_1, nm	N_1, m^{-3}	D_2, nm	N_2, m^{-3}
Initial state	162	$5.3 \cdot 10^{17}$	44	$5.1 \cdot 10^{20}$
After exposure to hydrostatic pressure $P = 1$ GPa $= 10$ kbar at a temperature of 293 K for 10 min	110	$5.6 \cdot 10^{17}$	35	$5.3 \cdot 10^{20}$
After annealing at a temperature of 510 K for 5.5 h	130	$5.2 \cdot 10^{17}$	33	$4.9 \cdot 10^{20}$
After annealing under load $\sigma = 0.8\sigma_r$ at a temperature of 510 K for 5.5 h	114	$5.1 \cdot 10^{17}$	30	$6.1 \cdot 10^{20}$

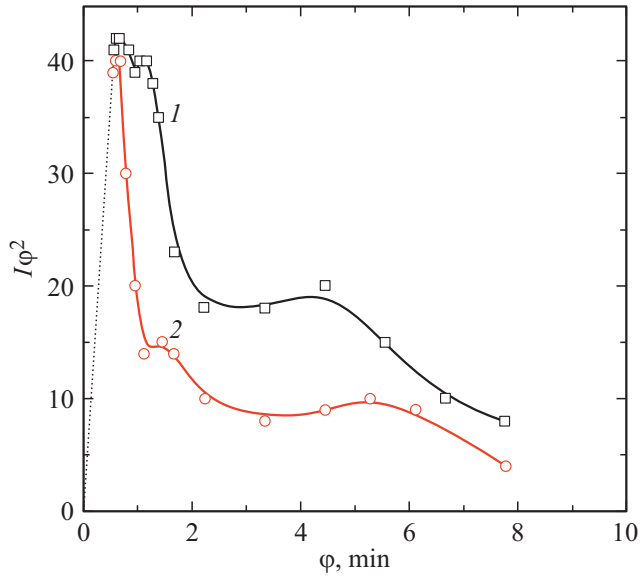

Figure 2. Second invariant of the $I\varphi^2$ scattering indicatrix, where I is scattering intensity, φ is scattering angle, for the $Ni_{82.1}Cr_{7.8}Si_{4.6}Fe_{3.1}Mn_{0.3}Al_{0.1}Cu_{<0.1}B_2$ amorphous alloy in the initial state (1) and after exposure to high hydrostatic pressure (2).

Guinier method [18] showed that this effect is associated with a decrease in the size of inhomogeneities.

Thus, the information on the healing effect of pressure and annealing on the sizes of regions of reduced density (in the extreme case — nanopores) obtained for amorphous tapes with a thickness of $\sim 70\,\mu$m has confirmed the previously obtained results for thinner (with a thickness of $20-30\,\mu$m) tapes of amorphous alloys based on Fe, Co [6,14].

To more accurately determine the parameters of inhomogeneities, especially their concentrations, using the SAXS method, their shape was determined. Based on the analysis of the data obtained by the SAXS method with the X-ray beam oriented along and across the amorphous tape with a thickness of $\sim 70\,\mu$m, it was found that inhomogeneities (as for tapes with a thickness of $20\,\mu$m [6]) have an ellipsoidal, close to spherical, shape, with the short and long axes of the ellipse being related as 1.12/1.14. In this regard, in further analysis of the SAXS data, carried out according to [18,19], the size of discontinuities was considered close to their reduced diameter, and the discontinuities themselves were considered as nanopores.

The values of the size and concentration of discontinuities in the initial (after UFQ) amorphous alloy and in the same alloy after exposure to annealing, annealing under load and hydrostatic pressure, obtained taking into account the above refinements, are given in Table 2.

The table shows that the average pore sizes after UFQ are approximately 160 and 40 nm. After exposure to annealing and pressure, the sizes of large and small discontinuities decrease by approximately 30%.

It has been established (Table 2) that the concentration of „small“ discontinuities is almost four orders of magnitude greater than that of „large“ discontinuities, and due to this

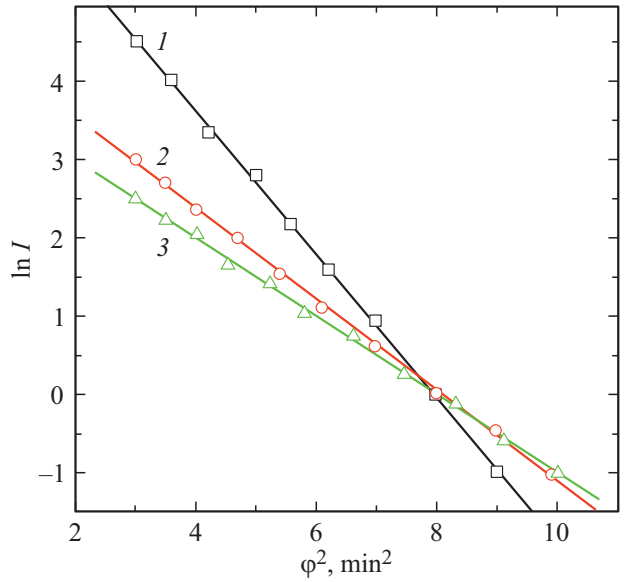

Figure 3. Scattering indicatrix for the $Ni_{82.1}Cr_{7.8}Si_{4.6}Fe_{3.1}Mn_{0.3}Al_{0.1}Cu_{<0.1}B_2$ amorphous alloy in the Guinier approximation for one of the pore fractions in the initial state (*1*), after annealing at a temperature of 510 K (*2*) and after annealing at a temperature of 510 K under load (*3*).

their contribution to the total excess free volume is the main one ($\geq 90\%$). To clarify the reasons for this effect, the distribution of „large“ inhomogeneities over the thickness of the amorphous tape was studied by the SAXS method. It has been established that in tapes with a thickness of $\sim 70\,\mu$m, large discontinuities are observed almost only in the surface layer (with a thickness of $\sim 4\,\mu$m), which does not come into contact with the cooling disk during UFQ. (For samples of amorphous alloys with a thickness of $\sim 30\,\mu$m, such an outer surface layer has a thickness of $\sim 2\,\mu$m; the nature of this effect is considered in [6]).

When analyzing the data in Table 2, also the following features of the effect of thermomechanical treatment on the properties of amorphous alloys should be noted.

A decrease in the size of discontinuities during thermomechanical processing leads to a decrease in the elastic energy associated with the EFV. According to [22], the decrease in elastic energy in amorphous alloys is most intense on the surface, where, as it has been established in this study, the effect of an increased concentration of „large“ discontinuities is observed. The above analysis suggests that the surface „smoothing“ discovered by the atomic-force microscopy after thermomechanical treatment is associated with the evolution of the EFV [15].

Also, it can be seen from Table 2 that although the concentration of „large“ and „small“ discontinuities practically does not change during processing, for large ones there is a trend towards decrease in their concentration, and small discontinuities demonstrate a trend toward slight increase. In other words, after thermomechanical treatment there is some leveling in size.

Thus, it can be assumed that thermomechanical treatment not only leads to an improvement in mechanical (Table 1) and magnetic [23] characteristics and to an increase in resistance to microfracture [13], but also contributes to the transfer of the amorphous alloy from a nonequilibrium to a more stable state due to the healing of the EFV.

For practice, both the data on the study of amorphous alloys of increased size (thickness) and the choice of methods and sequence of thermomechanical treatments of the alloy obtained after UFQ can be useful.

Conflict of interest

The authors declare that they have no conflict of interest.

References

[1] K. Suzuki, H. Fujimori, K. Hashimoto. Amorfnye metally, Metallurgiya, M., (1987), 328 s. (in Russian).
[2] G.E. Abrosimova, A.S. Aronin, S.V. Dobatkin, I.I. Zverkova, D.V. Matveev, O.G. Rybchenko, E.V. Tatyanin. FTT **49**, *6*, 983 (2007). (in Russian).
[3] N. Iturriza, M. Nazmunnahar. J. Nanosci. Nanotechnol. **12**, *6*, 5071 (2012).
[4] M. Dośpial, M. Nabialek, M. Szota, P. Pietrusiewicz, K. Gruszka, K.Bloch. Acta Phys. Pol. A **126**, *1*, 170 (2014).
[5] A.M. Glezer, B.V. Molotilov. Struktura i mekhanicheskie svoistva amorfnykh splavov, Metallurgiya, M., (1992). 206 s. (in Russian).
[6] V.I. Betekhin, A.M. Glezer, A.G. Kadomtsev, A.Yu. Kipyatkova. FTT **40**, *1*, 85 (1998). (in Russian).
[7] D. Turnbull, M.H. Cohen. J. Chem. Phys. **34**, *1*, 120 (1961).
[8] M.L. Falk, J.S. Langer. Phys. Rev. E **57**, *6*, 7192 (1998).
[9] L. Anand, C. Su. J. Mech. Phys. Solids **53**, *6*, 1362 (2005).
[10] J.-Z. Jiang, D. Hofmann, D.J. Jarvis, H.-J. Fecht. Adv. Eng. Mater. **17**, *6*, 761 (2015).
[11] Metastabilnye i neravnovesnye splavy / Eds. Yu.V. Efimov, Metallurgiya, M., (1988). 382 s. (in Russian).
[12] V.I. Betekhin, A.G. Kadomtsev, T.V. Larionova, M.V. Narykova. MiTOM **10**, *712*, 38 (2014). (in Russian).
[13] A.M. Glezer, V.I. Betekhin. FTT **38**, *6*, 1784 (1996). (in Russian).
[14] V.I. Betekhin, A.G. Kadomtsev, O.V. Tolochko. FTT **43**, *10*, 1815 (2001). (in Russian).
[15] P.N. Butenko, V.I. Betekhin, V.E. Korsukov, A.G. Kadomtsev, M.V. Narykova. FTT **62**, *11*, 1781 (2020). (in Russian).
[16] Ya.I. Frenkel. Vvedeniye v teoriyu metallov, Nauka, L., (1972), 424 s. (in Russian).
[17] S.P. Nikanorov, B.K. Kardashev. Uprugost' i dislokatsionnaya neuprugost' kristallov, Nauka, M., (1985), 254 s. (in Russian).
[18] A. Guinier, G. Fournet. Small-Angle Scattering of X-Rays. Wiley, N.Y. (1955). 268 p.
[19] D.I. Svergun, L.A. Feigin. Rentgenovskoe i neitronnoe malouglovoe rasseyanie, Nauka, M., (1986), 198 s. (in Russian).
[20] V.I. Betekhin, A.G. Kadomtsev, O.V. Amosova. Izv. AN. Ser. fiz. **67**, *6*, 818 (2003). (in Russian).
[21] V.I. Betekhin, A.G. Kadomtsev, S.Yu. Veselkov, Yu.R. Dal. FTT **45**, *4*, 42 (2003). (in Russian).
[22] Metallichasie styokla. Ionnaya struktura, elektronny perenos i kristallizatsiya / Eds. G. Bek, G. Gyunterodt, Mir, M., 1983, 376 s. (in Russian).
[23] A.I. Slutsker, V.I. Betekhin, A.G. Kadomtsev, O.V. Tolochko. ZhTF **76**, *12*, 57 (2006). (in Russian).

Translated by Y.Alekseev